TiO$_2$/PVDF hollow fiber membranes for the separation of dyes and salts (NaCl and Na$_2$SO$_4$) during textile wastewater treatment

Huiqiang Liu[a], Yingbo Chen[a],*, Xiaoyu Hu[b], Kai Zhang[a], Bowen Cheng[c], Dongqing Liu[a], Yufeng Zhang[a], Sankar Nair[a,d]

[a]*School of Materials Science and Engineering, State Key Laboratory of Separation Membranes and Membrane Processes, Tianjin Polytechnic University, Tianjin 300387, China, Tel. +86 22 83955357; email: chenyingbo@tjpu.edu.cn (Y. Chen)*
[b]*State Key Laboratory of Membrane Materials and Membrane Applications, Tianjin Motimo Membrane Technology Co. Ltd., Tianjin 300042, China*
[c]*School of Textile, Tianjin Polytechnic University, Tianjin 300387, China*
[d]*School of Chemical and Biomolecular Engineering, Georgia Institute of Technology, Atlanta 30332, USA*

ABSTRACT

In this work, a titanium oxide/polyvinylidene fluoride (TiO$_2$/PVDF) hollow fiber membrane was fabricated to fractionate the dye and Na$_2$SO$_4$ produced in textile wastewater. This hollow fiber membrane offered high retention of Congo red and methylene blue dyes with little rejection of Na$_2$SO$_4$. More importantly, the membrane was obtained using single orifice spinneret through a simple, rapid, and less expensive procedure. Meanwhile, the membrane exhibited good hydrophilicity, flux recovery ratio, and long-term stability, when appropriate blending of TiO$_2$ nano-particles was conducted. These results highlight interesting potential applications, and open new directions toward the designing of efficient functional hollow fibers for effective fractionation of dye and Na$_2$SO$_4$ for the treatment of textile wastewater.

Keywords: PVDF; Hollow fiber membrane; Textile wastewater; Titanium dioxide

1. Introduction

China produces around 2.37×10^{10} t of textile wastewater every year [1], which is one of the most challenging industrial problems to deal with due to the toxicity of azo dyes and high salinity. Conventional treatment methods, such as adsorption, coagulation, advanced oxidation, and biological degradation process can directly convert azo dyes present in wastewater into bioelectricity [2–5]. However, this approach makes it difficult to recover valuable residual dyes and salts. Considering the presence of 6.0 wt% NaCl or 5.6 wt% Na$_2$SO$_4$ in textile wastewater [6–8], separation of these salts is considered a valuable and sustainable practice.

Pressure-driven membrane technology can potentially achieve more sustainable operation by fractionation of the dye and salt mixtures with subsequent recycling of the recovered dye and salts [6,9].

During the last few years, intensive research was done on the preparation of hollow fibers to separate salts from dye wastewater as the methods used included layer-by-layer self-assembly technique [10–13] and coating a layer onto a commercial ultrafiltration (UF) hollow fibers [14,15]. However, these methods together with the multistep production process led to an increase in the production time and costs [16–18]. Sometimes, in harsh environments containing organic solvents, weak interactions between the support and active layer result in the peeling of active layer from the support [19–21]. Therefore, it is essential to develop a simple preparation method, and optimize its operating conditions.

* Corresponding author.

Chen et al. [22] put forward a novel formation method for hollow fiber membranes (HFMs), which was based upon a dual pore formation mechanism. The HFMs were spun through a single orifice spinneret, and can be used for separating dyes. Fashandi et al. [23] developed HFMs using single orifice spinneret, which were free of micro-voids.

In this work, single orifice spinneret method has been used to prepare HFMs for separating salt from dye wastewater.

Polyvinylidene fluoride (PVDF) offers many unique and prominent advantages, including good membrane forming ability, thermal stability, excellent chemical resistance, good mechanical strength, and antioxidation activity. Due to these advantages, PVDF is widely used as a promising membrane forming material [24,25]. Beside these advantages, PVDF is also known as a hydrophobic material [26,27]. In the present work [28–31], TiO_2 nano-particles were blended to enhance the performance of hydrophilic HFMs.

2. Experimental setup

2.1. Materials and chemicals

PVDF (FR 904) was obtained from Shanghai 3F New Material Co., Ltd., China. N,N-dimethyl acetamide (DMAc; analytical reagent grade), and hydrochloric acid (HCl; analytical reagent grade) were purchased from Sinopharm Chemical Reagent Co., Ltd., China. Nano-sized TiO_2 (<40 nm) was purchased from Aladdin Industrial Co., China. Sodium borohydride ($NaBH_4$) was obtained from Tianjin Guangfu Fine Chemical Research Institute, China. All chemicals were purchased and used without further purification. Congo red and methylene blue were purchased from Tianjin Kermel Chemical Reagent Co., Ltd., China.

2.2. Membrane preparation

First, a certain amount of TiO_2 and 0.8 g $NaBH_4$ were dispersed in 78 g DMAc, and sonicated for 30 min to achieve an adequate dispersion. Then, 22 g PVDF was dissolved in the above solution with continuous stirring at 60°C for 10 h. After the degasification, the achieved homogeneous solution was transferred to an injection syringe. Membranes were prepared with the TiO_2 contents (compared with PVDF) of 0, 0.5, 1, and 5 wt%.

The PVDF HFMs were spun through a single orifice spinneret at the extrusion rate of 0.3 mL/min using a syringe pump [22] (1.54 mm inner diameter; horizontal to the water bath), which was directly immersed in the coagulation bath. The coagulation bath was divided into two sections. The first section was filled with distilled water (15 cm length), while the second section contained aqueous HCl solution (pH = 1.80) whose temperature was maintained at 25°C throughout the spinning process. The HFMs were kept in the coagulation bath. The prepared HFMs were immersed in deionized (DI) water for 24 h to remove the residual solvent in the membranes, and then successively immersed in aqueous glycerol solutions (30, 50, and 70 wt%) for 4 h in each concentration. The membranes were then dried in air at room temperature to make the test modules.

2.3. Membrane characterization

The surface morphology and the cross section of the hollow fiber were studied using scanning electron microscopy (SEM, S-4800, Hitachi, Japan). The membranes were cryogenically fractured in liquid nitrogen to obtain the cross-sections. Both surface and cross-section of the membranes were sputtered with gold. The elements and contents on membrane surface were examined using energy dispersive spectrometer (EDS) (Oxford INCA X-Max, UK). The membrane surface roughness was measured using atomic force microscope (Model: 5500 AFM, Agilent Technologies, USA). The water contact angle was measured using a dynamic contact angle tensiometer (DSA-100, KRUSS, Germany). To minimize the experimental errors, contact angles were averaged for at least five measurements of different locations of the membrane. The mechanical properties of the produced fibers were evaluated using single yarn fiber strength tester (model LLY-06). The initial distance between the clamps and the stretching rate were adjusted to be 2.5 cm and 10 mm/min, respectively. For each sample, five measurements were carried out, and the mean value was reported. The streaming potential measurements were performed using a SurPASS (Anton Paar, Graz, Austria) to measure the zeta potentials of the membrane surface. In addition, potassium chloride (1 mM) was used as the electrolyte, whereas hydrochloric acid and potassium hydroxide were used for titration.

2.4. Measurement of membrane separation properties

Membrane permeation experiments were performed using a laboratory scale cross-flow filtration apparatus. Before testing, the HFMs were pre-pressurized to 0.1 MPa pressure for 1 h with DI water to reach a stable state. The pure water flux for the HFM was measured by employing DI water as the feed, and was calculated using Eq. (1) [32]:

$$J_w = Q/\Delta PA \tag{1}$$

where Q stands for the volumetric permeation rate of pure water (L/h), ΔP is the trans-membrane pressure (bar), and A is the effective area of the HFMs (m^2).

The HFMs were applied to remove different dye molecules. The dye rejections and the permeate fluxes of the HFMs were measured using the same filtration apparatus. The dye concentrations were measured using an ultraviolet-visible spectrophotometer at the maximum absorption wavelength of each dye [33]. All the experimental measurements of the rejection rates and fluxes were performed at least three times, and average values were reported in this study.

The observed solute rejection, R_s, was evaluated using Eq. (2).

$$R_s(\%) = (C_f - C_p)/C_f \times 100 \tag{2}$$

where C_p and C_f are the solute concentrations in permeate and feed streams, respectively. The concentrations of NaCl and Na_2SO_4 were obtained by measuring the conductivity of aqueous solutions using a conductivity meter (DDSJ-308A, Cany Precision Instruments, China) and comparing the calibration plot drawn between the salt concentration

and conductivity. All results presented are average values with standard deviation calculated from at least three samples of each membrane type.

3. Results and discussion

3.1. Morphology of the hollow fiber membrane

The morphologies of PVDF and TiO_2/PVDF HFMs were observed using SEM. The morphologies of the cross-sections of HFMs are shown in Figs. 1(A) and (B), which illustrate that the macro-voids grew and became run-through at lower TiO_2 concentrations. However, after the addition of TiO_2 nano-particles, the cross-sectional morphologies of

TiO_2/PVDF HFMs changed from finger-like to sponge-like structures. Yang et al. [35] have reported similar results in their work. These results indicated that the addition of TiO_2 particles had a significant influence on the structure of membranes. The increase in viscosity of the dope due to the addition of TiO_2 particles slowed down the exchange rate of solvent/non-solvent, and tended to a delayed de-mixing process, thus resulting in the suppression of macro-voids [34]. Furthermore, EDS was applied to investigate the distribution of the TiO_2 particles on the cross-section of the membranes, the results of which are shown in Fig. 1(D). The EDS spectrum shows that the TiO_2 particles were uniformly distributed in the membranes.
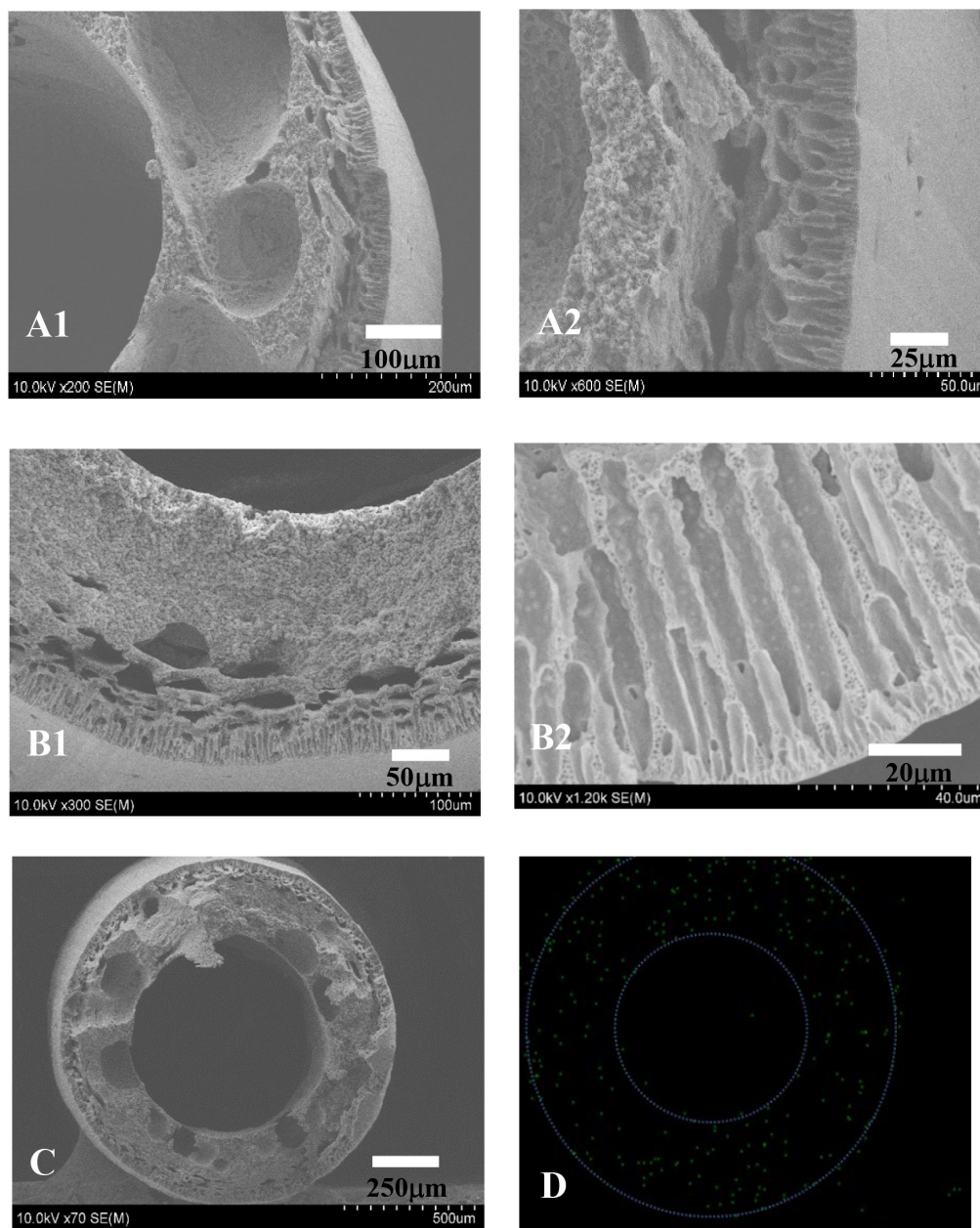
Fig. 1. SEM images and EDS of the hollow fiber membrane. (A) PVDF hollow fiber membrane, (B) 0.5 wt% TiO_2/PVDF hollow fiber membrane, (C) 0.5 wt% TiO_2/PVDF hollow fiber membrane, and (D) EDS (Ti) of membrane in images (C).

3.2. Effect of TiO₂ content

Fig. 2 shows the effect of addition of TiO_2 on the flux of pure water and rejection of Congo red for the HFMs. When the content of TiO_2 was increased from 0 to 0.5 wt%, both the membrane flux and the rejection rate of Congo red increased. However, when the content of TiO_2 was increased from 0.5 to 5 wt%, the membrane flux increased, while the rejection rate of Congo red decreased, which might be due to some large pores formed on the membrane surface due to the aggregates of TiO_2 nano-particles. Yang et al. [35] studied the effect of addition of TiO_2 on the morphologies and properties of polysulfone UF membranes, and reported that the pore radius increased at higher TiO_2 content, which was attributed to the aggregation of nano-particles that enhanced the formation of larger pores. In order to achieve a relatively high removal rate, the content of TiO_2 was fixed at 0.5 wt% during the membrane preparation experiments.

3.3. Atomic force microscopy analysis

Fig. 3 shows the three-dimensional surface AFM images of PVDF membrane surfaces. The roughness R_a (the roughness average) was obtained using the AFM analysis software in the scanning area of 4 μm × 4 μm. It was observed that the roughness of PVDF membrane was larger than that of the TiO_2/PVDF membrane. It is well known that the membrane with smoother surface has greater antifouling capability. The membrane fouling trend increases with the roughness owing to the contaminants accumulating on the rough membrane surface [36].

3.4. Zeta potential analysis

Membranes surface charge has a significant influence on the fouling and separation properties of membranes [37,38]. The changes in zeta potential of membranes with pH are presented in Fig. 4. It was shown that the zeta potential of all the membranes decreased with the increase in pH value of the solution. However, the zeta potential of 0.5 wt% TiO_2/PVDF HFM exhibited stronger positive zeta potentials under acidic conditions and stronger negative zeta potentials under basic conditions, whereas a point of zero potential was observed at the pH of around 5.8, which is in accordance with the results

reported by Li et al. [39]. More importantly, stronger positive and negative zeta potentials were conducive in controlling the fouling phenomenon by changing the pH of solutes. This way, the adsorption and deposition of foulants on the membrane surface can be controlled.
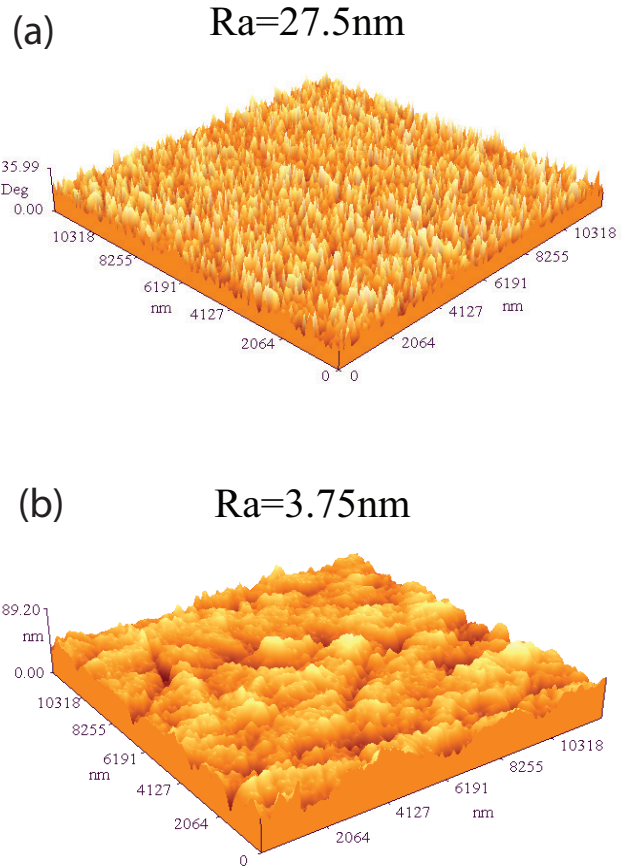
Fig. 3. AFM three-dimensional surface images of the hollow fiber membranes.
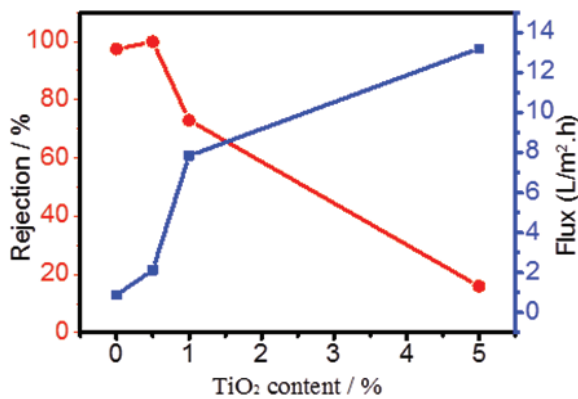
Fig. 2. Effect of TiO₂ content on the performance of membranes.
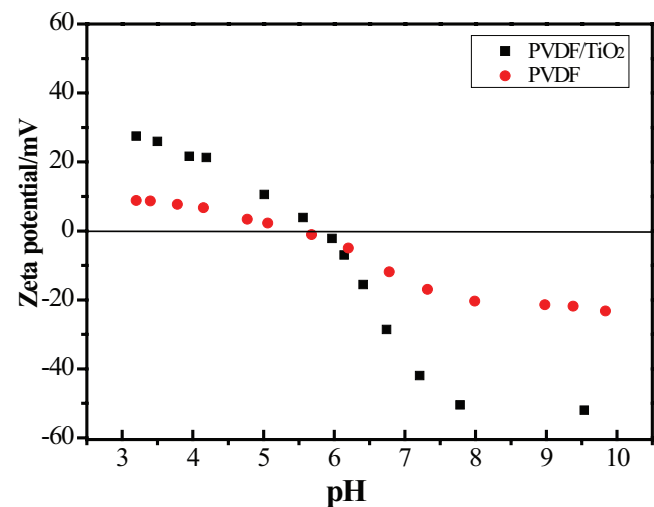
Fig. 4. Zeta potential of membranes as a function of pH value.

3.5. Contact angle analysis

The contact angles of the membranes were measured to evaluate their hydrophilic property. It was observed that the addition of TiO_2 led to a decrease in contact angles (Fig. 5). The values of contact angles for PVDF and 0.5 wt% TiO_2/PVDF membranes were found to be 84° ± 0.8° and 80° ± 0.7°, respectively. This indicated that the membrane hydrophilicity improved due to the addition of TiO_2 nano-particles. The contact angle increased with further addition of TiO_2, which may be because of the agglomeration of TiO_2, leading to a relatively coarser surface. Both the surface charge and hydrophobicity can obviously increase the antifouling property of membranes. In a hydrophilic membrane, a water layer is formed on the hydrophilic membrane surface through hydrogen bonding between the membrane and water molecules, which can reduce the adhesion of pollutants to hydrophilic membrane surfaces [40].

3.6. Mechanical properties of the membranes

In industrial applications of membranes, mechanical properties are very important for long-term stable operation. Fig. 6 shows the mechanical stability of PVDF and TiO_2/PVDF HFMs in terms of their stress–strain curves. The PVDF membrane possessed a typical inferior mechanical stability with a tensile strength of 3.48 MPa, along with the elongation at break of ca. 11.8%. When the TiO_2 content was increased from 0% to 0.5%, the tensile strength increased from 3.48 to 4.09 MPa, respectively, indicating that the introduction of TiO_2 nano-particles could substantially boost the mechanical properties of HFMs. The addition of nano-particles, suppression of macro-voids, and interactions between the inorganic particles and polymers resulted in an increase in the mechanical strength of the membranes [34]. These results were found to be consistent with those obtained from the SEM analysis. However, excessive amounts of TiO_2 easily caused the particles to aggregate and disperse non-uniformly in the polymer matrix. This resulted in many stress convergence points in the membrane system due to the action of external force, eventually leading to the weakening of mechanical stability of the membranes. Therefore, the optimum content of titanium oxide was determined to be 0.5 wt%.
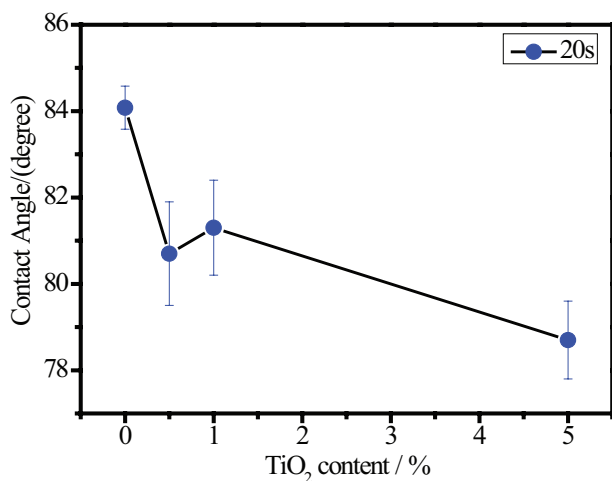
3.7. Membrane separation properties

Based upon the results presented in section 3.6, the 0.5 wt% TiO_2/PVDF HFM was used to investigate the separation properties. The water fluxes and salt rejections of the HFMs are presented in Table 1. The results show that the prepared HFMs exhibited an average water flux of 1.90 L/m² h, and NaCl and Na_2SO_4 rejections of 4.8% and 14.0%, respectively, for 1,000 mg/L aqueous solution of each salt under 1 bar pressure.

Submerged filtration tests were performed with different dye solutions employing HFMs. It was found that all the permeate streams were nearly colorless (Fig. 7) during the filtration process. The dye removals and permeate fluxes in submerged filtration of 50 mg/L dye solution are presented in Table 1. The results show that, under the pH of 7.0 and trans-membrane pressure of 1 bar, the HFMs can effectively remove dyes from aqueous solutions. The removals of methylene blue and Congo red are nearly 100%. It is well known that the rejection characteristic of the charged HFMs for charged solutes is mainly determined by both the effects of steric hindrance and electrostatic interactions [44]. Therefore, Congo red with relatively higher molecular weight will be rejected more efficiently by the negatively charged membrane. Methylene blue has a lower molecular weight. The cationic dyes will be adsorbed on negatively charged membranes, and block the membrane pores. Therefore, the permeability will be lower than that for the Congo red solution.
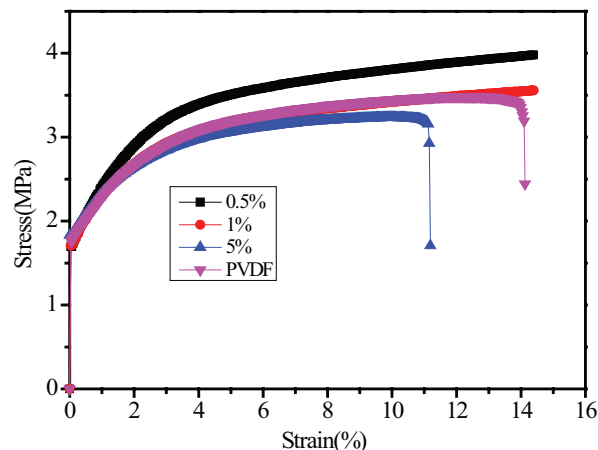
Fig. 6. Stress–strain curves for the PVDF hollow fiber membranes.

Table 1
Performance of 0.5% TiO_2/PVDF hollow fiber membrane

Retained matters	Permeate flux (L/m² h)	Rejection (%)
Congo red[a]	1.61 ± 0.30	99.99 ± 0.01
Methylene blue[a]	1.28 ± 0.25	99.9 ± 0.05
Na_2SO_4[b]	1.90 ± 0.30	14.0 ± 0.54
NaCl[b]	1.90 ± 0.28	4.8 ± 0.36

[a]Tested with aqueous dye solution 50 mg/L under the trans-membrane pressure of 1 bar, temperature of 25°C, and pH of 7.0.
[b]Tested with aqueous salt solution 1,000 mg/L under the trans-membrane pressure of 1 bar, temperature of 25°C, and pH of 7.0.

Fig. 5. Water contact angle of PVDF hollow fiber membrane.

Higher dye rejection and lower salt rejection can be obtained with the hollow fiber membranes in this study compared with other hollow fiber membranes as listed in Table 2. The higher dye separation efficiency and lower salt rejection mean that the TiO$_2$/PVDF HFM has a good potential application in the separation of salts from dye wastewater.

Long-term stability is another vital factor to explore the performance of HFMs. In the present work, long-term dye removal test was conducted to investigate the stability of HFMs during the submerged filtration tests of dye solutions.
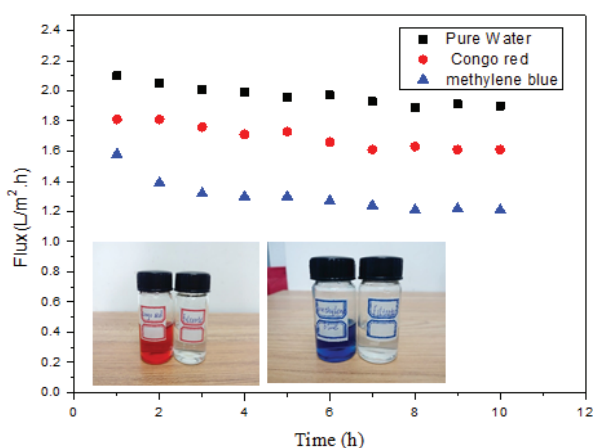
Fig. 7. Membrane permeates fluxes for dye solutions and membrane rejections for dyes (dye concentration: 50 mg/L).

Fig. 8. Changes in dye rejection and water flux with filtration time for the hollow fiber membranes filtrated with 50 mg/L methylene blue aqueous solution at 1 bar, 25°C, and pH of 7.

Fig. 8 illustrates the changes in water flux and dye removal for the studied membranes during a 30-h continuous filtration of 50 mg/L methylene blue solution under the conditions of 1 bar, 25°C, and pH of 7.0. Every 3 h, the membranes were rinsed for 30 min. The dye removal remained nearly constant at around 99.9% during the whole filtration process. The water flux declined slightly within the first 3 h, and was recovered by the washing process. The small dye particles were likely to be adsorbed on the pore walls, which resulted in the decline of permeate flux at the early stage. However, after washing the membranes, the permeate flux regained a high value. The results of long-term test indicated that the HFMs developed in this study possessed good long-term stability in submerged filtration of aqueous dye solutions.

4. Conclusions

In this work, TiO$_2$ nano-particles were used to prepare TiO$_2$/PVDF HFMs using a novel single orifice spinneret method. The HFMs showed excellent hydrophilic and mechanical properties. With the addition of 0.5% TiO$_2$ nano-particles, the HFMs demonstrated a good performance in separating the salt from dye wastewater. The membranes showed NaCl and Na$_2$SO$_4$ rejections of 4.8% and 14.0%, respectively, and almost completely retained methylene blue and Congo red. The higher dye separation efficiency and lower salt rejections indicated that the TiO$_2$/PVDF HFMs have promising application potential with regards to the separation of salt from dye wastewater.

References

[1] X.A. Ning, M.Q. Lin, L.Z. Shen, J.H. Zhang, J.Y. Wang, Y.J. Wang, Z.Y. Yang, J.Y. Liu, Levels, composition profiles and risk assessment of polycyclic aromatic hydrocarbons (PAHs) in sludge from ten textile dyeing plants, Environ. Res., 132 (2014) 112–118.
[2] J. Sun, Y.Y. Hu, Z. Bi, Y.Q. Cao, Simultaneous decolorization of azo dye and bioelectricity generation using a microfiltration membrane air-cathode single chamber microbial fuel cell, Bioresour. Technol., 100 (2009) 3185–3192.
[3] S. Kalathil, J. Lee, M.H. Cho, Granular activated carbon based microbial fuel cell for simultaneous decolorization of real dye wastewater and electricity generation, New Biotechnol., 29 (2011) 32–37.

Table 2
Comparisons of the separation performances of various hollow fiber membranes with those tested in this work

Author	Manufacture	Dyes	Dyes molecular weight (g/mol)	Dyes removal (%)	Salts removal (%)
Zheng [41]	Coating	Crystal violet	408.0	99.2	35.4
Wei [42]	Interfacial polymerization	Acid red B	502.4	99.9	39.8
Mondal and De [43]	Interfacial polymerization	Reactive dyes	–	99.8	42.0
This work	One-step spinning	Methylene blue	319.9	99.99	4.8

[4] G. Mohanakrishna, S.V. Mohan, P. Sarma, Bio-electrochemical treatment of distillery wastewater in microbial fuel cell facilitating decolorization and desalination along with power generation, J. Hazard. Mater., 177 (2010) 487–494.

[5] C.H. Feng, F.B. Li, H.J. Mai, X.Z. Li, Bio-electro-Fenton process driven by microbial fuel cell for wastewater treatment, Environ. Sci. Technol., 44 (2010) 1875–1880.

[6] J. Lin, W. Ye, H. Zeng, H. Yang, J. Shen, S. Darvishmanesh, P. Luis, A. Sotto, B. Vander Bruggen, Fractionation of direct dyes and salts in aqueous solution using loose nanofiltration membranes, J. Membr. Sci., 477 (2015) 183–193.

[7] B. Van der Bruggen, B. Daems, D. Wilms, C. Vandecasteele, Mechanisms of retention and flux decline for the nanofiltration of dye baths from the textile industry, Sep. Purif. Technol., 22 (2001) 519–528.

[8] I. De Vreese, B. Van der Bruggen, Cotton and polyester dyeing using nanofiltered wastewater, Dyes Pigm., 74 (2007) 313–319.

[9] X. Chen, Y. Zhao, J. Moutinho, J. Shao, A.L. Zydney, Y. He, Recovery of small dye molecules from aqueous solutions using charged ultrafiltration membranes, J. Hazard. Mater., 284 (2015) 58–64.

[10] C. Liu, L. Shi, R. Wang, Cross linked layer-by-layer polyelectrolyte nano filtration hollow fiber membrane for low-pressure water softening with the presence of SO_4^{2-} in feed water, J. Membr. Sci., 486 (2015) 169–176.

[11] D. Menne, J. Kamp, J.E. Wong, M. Wessling, Precise tuning of salt retention of backwashable polyelectrolyte multilayer hollow fiber nanofiltration membrane, J. Membr. Sci., 499 (2016) 396–405.

[12] J. de Grooth, D.M. Reurink, J. Ploegmakers, W.M. de Vos, K. Nijmeijer, Charged micropollutant removal with hollow fiber nanofiltration membranes based on polycation/polyzwitterion/polyanion multilayers, ACS Appl. Mater. Interfaces, 6 (2014) 17009–17017.

[13] S. Ilyas, J. de Grooth, K. Nijmeijer, W.M. de Vos, Multifunctional polyelectrolyte multilayers as nanofiltration membranes and as sacrificial layers for easy membrane Cleaning, J. Colloid Interface Sci., 446 (2015) 386–393.

[14] A. Verliefe, E. Cornelissen, G. Amy, B. Van der Bruggen, H. vanDijk, Priority organic micropollutants in water sources in Flanders and the Netherlands and assessment of removal possibilities with nanofiltration, Environ. Pollut., 146 (2007) 281–289.

[15] Y.J. Jung, Y. Kiso, B. Adavih, R.A. Othman, A. Ikeda, K. Nishimura, K.S. Min, A. Kumano, A. Ariji, Rejection properties of aromatic pesticides with a hollow fiber NF membrane, Desalination, 180 (2005) 63–71.

[16] N. Peng, N. Widjojo, P. Sukitpaneenit, M.M. Teoh, G.G. Lipscomb, T.S. Chung, J.Y. Lai, Evolution of polymeric hollow fibers as sustainable technologies: past, present and future, Prog. Polym. Sci., 37 (2012) 1401–1424.

[17] C.R. Tavares, M. Vieira, J.C.C. Petrus, E.C. Bortoletto, F. Ceravollo, Ultrafiltration/complexation process for metal removal from pulp and paper industry wastewater, Desalination, 144 (2002) 261–265.

[18] W.G.J. van der Meer, J.C. van Dijk, Theoretical optimization of spiral-wound and capillary nanofiltration modules, Desalination, 113 (1997) 129–146.

[19] Y.F. Li, Y.L. Su, J.Y. Li, X.T. Zhao, R.N. Zhang, X.C. Fan, J.N. Zhu, Y.Y. Ma, Y. Liu, Z.Y. Jiang, Preparation of thin film composite nanofiltration membrane with improved structural stability through the mediation of polydopamine, J. Membr. Sci., 476 (2015) 10–19.

[20] Z. Jiaojiao, S. Yanlei, S. Xin, Z. Xueting, L. Yafei, Z. Runnan, J. Zhongyi, Dopamine composite nanofiltration membranes prepared by self-polymerization and interfacial polymerization, J. Membr. Sci., 465 (2014) 41–48.

[21] Z. Jun, L. Yu, L. Xiong, Y. Yin, W. Xuefen, Bioenabled interfacial polymerized on nanofibrous scaffold as composite nanofiltration membrane, Adv. Mater. Res., 482–484 (2012) 565–568.

[22] Y.B. Chen, X.P. Hu, X.Y. Hu, Y.F. Zhang, Polymeric hollow fiber membranes prepared by dual pore formation mechanism, Mater. Lett., 143 (2015) 315–318.

[23] H. Fashandi, K. Zarrini, M. Youssefi, Synergistic contribution of spinneret diameter and physical gelation to develop macrovoid-free hollow fiber membranes using single orifice spinneret, Ind. Eng. Chem. Res., 54 (2015) 7728–7736.

[24] A. Fadaei, A. Salimi, M. Mirzataheri, Structural elucidation of morphology and performance of the PVDF/PEG membrane, J. Polym. Res., 21 (2014) 545.

[25] H. Sardarabadi, S.M. Mousavi, E. Saljoughi, Removal of 2-propanol from water by pervaporation using poly(vinylidene fluoride) membrane filled with carbon black, Appl. Surf. Sci., 368 (2016) 277–287.

[26] Z. Wang, H. Yu, J. Xia, F. Zhang, F. Li, Y. Xia, Y. Li, Novel GO-blended PVDF ultrafiltration membranes, Desalination, 299 (2012) 50–54.

[27] C. Zhao, X. Xu, J. Chen, F. Yang, Effect of graphene oxide concentration on the morphologies and antifouling properties of PVDF ultrafiltration membranes, J. Environ. Chem. Eng., 1 (2013) 349–354.

[28] S.P. Albu, A. Ghicov, J.M. Macak, Self-organized, free-standing TiO_2 nanotube membrane for flow-through photocatalytic applications, Nano Lett., 7 (2007) 1286–1289.

[29] C.S. Ong, W.J. Lau, P.S. Goh, B.C. Ng, Preparation and characterization of PVDF–PVP–TiO_2 composite hollow fiber membranes for oily wastewater treatment using submerged membrane system, Desal. Wat. Treat., 53 (2015) 1213–1223.

[30] Y. Jafarzadeh, R. Yegani, Analysis of fouling mechanisms in TiO_2 embedded high density polyethylene membranes for collagen separation, Chem. Eng. Res. Des., 93 (2015) 684–695.

[31] A. Qin, X. Li, X. Zhao, D. Liu, C. He, Engineering highly hydrophilic PVDF membrane via binding TiO_2 nanoparticles and PVA layer onto membrane surface, ACS Appl. Mater. Interfaces, 7 (2015) 8427–8436.

[32] R. Wang, L. Shi, C.Y. Tang, S. Chou, C.Q. Qiu, A.G. Fanea, Characterization of novel forward osmosis hollow fiber membranes, J. Membr. Sci., 355 (2010) 158.

[33] X.Z. Wei, S.X. Wang, Y.Y. Shi, H. Xiang, J.Y. Chen, B.K. Zhu, Characterization of a positively charged composite nanofiltration hollow fiber membrane prepared by a simplified process, Desalination, 350 (2014) 44–52.

[34] L.Y. Yu, H.M. Shen, Z.L. Xu, PVDF–TiO_2 Composite hollow fiber ultrafiltration membranes prepared by TiO_2 sol–gel method and blending method, J. Appl. Polym. Sci., 113 (2010) 1763–1772.

[35] Y. Yang, H. Zhang, P. Wang, Q. Zheng, J. Li, The influence of nano-sized TiO_2 fillers on the morphologies and properties of PSF UF membrane, J. Membr. Sci., 288 (2007) 231–238.

[36] S.J. Oh, N. Kim, Y.T. Lee, Preparation and characterization of PVDF/TiO_2 organic–inorganic composite membranes for fouling resistance improvement, J. Membr. Sci., 345 (2009) 13–20.

[37] K.J. Kim, A.G. Fane, M. Nystrom, Evaluation of electroosmosis and streaming potential for measurement of electric charges of polymeric membranes, J. Membr. Sci., 116 (1996) 149–159.

[38] K. Rodemann, E. Staude, Electrokinetic characterization of porous membranes made from epoxidized polysulfone, J. Membr. Sci., 104 (1995) 147–155.

[39] X.P. Li, Y.B. Chen, X.Y. Hu, Y.F Zhang, L.J Hu., Desalination of dye solution utilizing PVA/PVDF hollow fiber composite membrane modified with TiO_2 nanoparticles, J. Membr. Sci., 471 (2014) 118–129.

[40] J.A. Brant, A.E. Childress, Colloidal adhesion to hydrophilic membrane surfaces, J. Membr. Sci., 241 (2004) 235–248.

[41] Y. Zheng, G. Yao, Q. Cheng, S. Yu, M. Liu, C. Gao, Positively charged thin-film composite hollow fiber nanofiltration membrane for the removal of cationic dyes through submerged filtration, Desalination, 328 (2013) 42–50.

[42] X. Wei, X. Kong, C. Sun, J. Chen, Characterization and application of a thin-film composite nanofiltration hollow fiber membrane for dye desalination and concentration, Chem. Eng. J., 223 (2013) 172–182.

[43] M. Mondal, S. De, Treatment of textile plant effluent by hollow fiber nanofiltration membrane and multi-component steady state modeling, Chem. Eng. J., 285 (2016) 304–318.

[44] B. Van der Bruggen, J. Schaep, D. Wilms, C. Vandecasteele, Influence of molecular size, polarity and charge on the retention of organic molecules by nanofiltration, J. Membr. Sci., 156 (1999) 29–41.